ACS Medicinal Chemistry Letters

Letter

pubs.acs.org/acsmedchemlett

Structure Guided Optimization, in Vitro Activity, and in Vivo Activity of Pan-PIM Kinase Inhibitors

Matthew T. Burger,*[,†] Wooseok Han,[†] Jiong Lan,[†] Gisele Nishiguchi,[†] Cornelia Bellamacina,[†] Mika Lindval,[†] Gordana Atallah,[†] Yu Ding,[†] Michelle Mathur,[†] Chris McBride,[†] Elizabeth L. Beans,[†] Kristine Muller,[†] Victoriano Tamez,[†] Yanchen Zhang,[†] Kay Huh,[†] Paul Feucht,[‡] Tatiana Zavorotinskaya,[‡] Yumin Dai,[‡] Jocelyn Holash,[‡] Joseph Castillo,[‡] John Langowski,[‡] Yingyun Wang,[‡] Min Y. Chen,[‡] and Pablo D. Garcia[‡]

[†]Global Discovery Chemistry/Oncology & Exploratory Chemistry, Novartis Institutes for Biomedical Research, 4560 Horton Street, Emeryville, California 94608, United States

[‡]Oncology Research, Novartis Institutes for Biomedical Research, 4560 Horton Street, Emeryville, California 94608, United States

Supporting Information

ABSTRACT: Proviral insertion of Moloney virus (PIM) 1, 2, and 3 kinases are serine/threonine kinases that normally function in survival and proliferation of hematopoietic cells. As high expression of PIM1, 2, and 3 is frequently observed in many human malignancies, including multiple myeloma, non-Hodgkins lymphoma, and myeloid leukemias, there is interest in determining whether selective PIM inhibition can improve outcomes of these human cancers. Herein, we describe our efforts toward this goal. The structure guided optimization of a singleton high throughput screening hit in which the potency against all three PIM isoforms was increased >10,000-fold to yield compounds with pan PIM K_is < 10 pM, nanomolar cellular potency, and in vivo activity in an acute myeloid leukemia Pim-dependent tumor model is described.

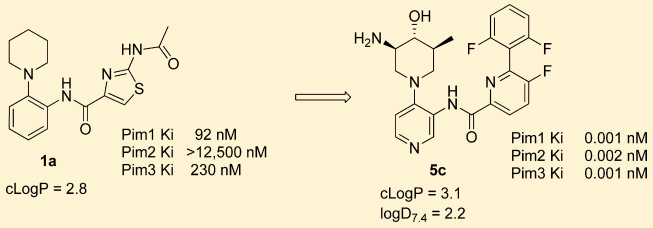

KEYWORDS: *Proviral insetion site in Moloney murine leukemia virus kinases inhibitors, Pim1 kinase inhibitor, Pim2 kinase inhibitor, Pim3 kinase inhibitor, pan-Pim kinase inhibitors*

Proviral insertion site of Moloney murine leukemia virus kinases, or PIM 1, 2, and 3 kinases are constitutively active serine/threonine kinases that normally function in the survival, proliferation, and differentiation of hematopoietic cells in response to growth factors and cytokines.[1,2] PIM's play redundant roles in oncogenesis and, therefore, suggest that a pan-PIM kinase inhibitor may be clinically useful.[3] In human disease, high expression and/or dysfunction of the three PIMs has been implicated in the progression of hematopoetic and solid tumor cancers.[1,2] In addition to cancer, PIM kinases have been reported to play a role in several autoimmune diseases.[4] Not surprisingly, PIM kinases have emerged as attractive therapeutic targets and have elicited several groups to investigate and report novel inhibitors of PIM[5−10] including the clinical compounds SGI-1776[6] and AZD1208,[7] Figure 1. Pim kinases share a high level of sequence homology within the family (>61%) and all share the unique feature of being the only kinases with a proline in the hinge,[11] which results in only one hydrogen bond interaction with ATP. As the ATP K_m for PIM2 is 10−100× lower than that for PIM1 and PIM3, cell active pan PIM inhibitors have been more challenging to identify than PIM 1/3 inhibitors. Herein, we describe potent and selective cell active inhibitors of all three PIM kinases. A representative of this compound series, **5c**, has suitable PK properties and was recently used to establish a PK/PD efficacy relationship in a PIM2 driven multiple myeloma xenograft model.[12] Here we also demonstrate efficacy in the AML EOL-1 xenograft model.

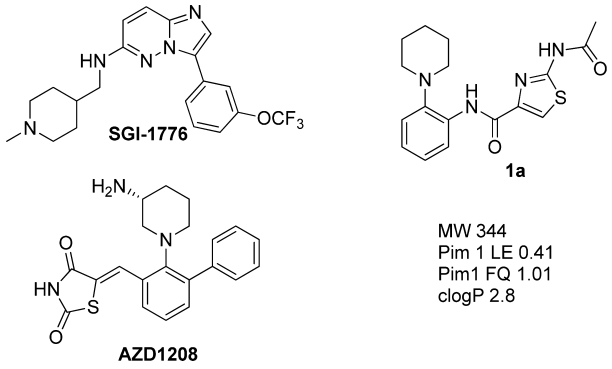

Figure 1. Pim clinical compounds and starting point **1a**.

Received: August 6, 2013
Accepted: October 12, 2013
Published: October 15, 2013

The starting point for our discovery efforts was the singleton high throughput screening hit **1a**. While of modest pan PIM potency, we followed up on it due to its low molecular weight (344), good PIM1 ligand efficiency (LE = 0.41, FQ = 1.01) and a presumed nonplanar ground state conformation for the ortho-substituted acylaniline moiety, which we reasoned might ultimately be beneficial with respect to physicochemical properties.

Prior to starting any synthetic chemistry efforts, a cocrystal structure of compound **1a** in PIM1 was obtained, Figure 2.[13]

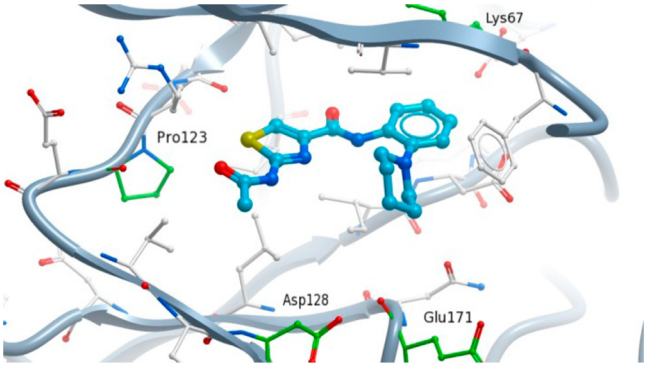

Figure 2. Structure of **1a** in PIM1.

We were intrigued by several aspects of the binding interactions (or lack thereof), which suggested multiple avenues to increase potency and, importantly, not necessarily increase the size or lipophilicity. First, there was no H bonding interaction to the hinge (or any other part of the protein). Second, the phenyl group was positioned in proximity to the catalytic Lys67. Third, the piperidine was in a chair conformation with well-defined vectors to access potential hydrogen bonding interactions in the acidic patch below and hydrophobic interactions to the glycine rich loop above. Additionally, the NH-acetyl substituent extended toward the hydrophobic lower hinge, making no hydrogen bonds. Furthermore, the central amide in the molecule made no hydrogen bonds as well, appearing to serve only as a rigid linker connecting the phenyl and thiazole rings.

Hit optimization efforts were initiated by variation of the piperidine (A ring), phenyl (B ring), and N−Ac thiazole (C ring) components of compound **1a**. PIM1−3 kinase activity was assessed initially in a Kinase-Glo assay, with [ATP] at or below ATP K_m for each isoform. As compound potency increased, vide infra, the assay format was changed to a high [ATP] Alphascreen format to extend the assay sensitivity. Compound enzymatic data is presented as K_is to allow comparison of activity of compounds run in the two assay formats. Removal of the N−Ac from the thiazole **1a** starting point yielded **1b** with >10× reduced potency, Table 1 . From this weakly potent compound lacking any extensions to the lower hinge, modifications in the C ring with heterocycles were surveyed. Of note, aminopyrazine **1c** increased potency relative to **1b** as well as demonstrating measurable PIM2 potency with no extenstion to the lower hinge and with a half unit reduction in cLogP. Modification of the phenyl B ring in **1a** targeted potential hydrogen bonding interactions with catalytic Lys67. Multipe heterocycles and amino or hydroxy substituted heterocycles gave marginal improvement in potency. However, it was noted that B ring pyridine **2b** maintained the potency of the lead **1a**, while having a 0.5 unit reduction in cLogP. Combination of the aminopyrazine C ring and pyridine B ring led to compound **3a** with a clogP of 1.9, a 3× improved potency against PIM1 and 3 and now measurable PIM2 potency (≥ 10× improvement). From **3a**, variation of the piperidine A ring with various amine and amide substituted

Table 1. Selected SAR for A, B, and C Ring Variations of 1a

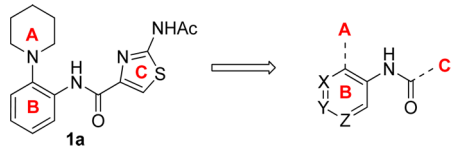

compd	A ring	B ring	C ring	PIM1 K_i (nM)	PIM2 K_i (nM)	PIM3 K_i (nM)	cLogP
1a	1-piperidyl	X,Y,Z = CH	2-NHAc-4-thiazolyl	92	>12,500	230	2.8
1b	1-piperidyl	X,Y,Z = CH	4-thiazolyl	1,800	>12,500	>12,500	2.9
1c	1-piperidyl	X,Y,Z = CH	3-NH_2, 2-pyrazinyl	460	7,000	1,500	2.5
1d	1-piperidyl	X,Y,Z = CH	3-NH_2, 2-pyridyl	3,300	>12,500	12,000	3.1
1e	1-piperidyl	X,Y,Z = CH	3-OH, 2-pyridyl	12,300	>12,500	>12,500	4.0
1g	1-piperidyl	X,Y,Z = CH	6-NH_2, 2-pyridyl	2,300	>12,500	11,000	2.8
1h	1-piperidyl	X,Y,Z = CH	2-imidazoyl	>12,500	>12,500	>12,500	2.4
2a	1-piperidyl	Y = N, X,Z = CH	2-NHAc-4-thiazolyl	59	6,300	140	2.3
2b	1-piperidyl	Z = N, X,Y = CH	2-NHAc-4-thiazolyl	61	>12,500	220	2.3
2c	1-piperidyl	X,Z = N, Y = CH	2-NHAc-4-thiazolyl	>12,500	>12,500	>12,500	1.6
2d	1-piperidyl	X,Z = N, Y = CNH_2	2-NHAc-4-thiazolyl	>12,500	>12,500	>12,500	1.6
2e	1-piperidyl	X = CH,Z = N,Y = CNH_2	2-NHAc-4-thiazolyl	1,000	>12,500	1,700	1.9
3a	1-piperidyl	Z = N, X,Y = CH	3-NH_2, 2-pyrazinyl	30	1,600	90	1.9
3b	1-piperazinyl	Z = N, X,Y = CH	3-NH_2, 2-pyrazinyl	810	>12,500	1,000	0.5
3c	4-(2-aminoacetyl)piperazin-1-yl	Z = N, X,Y = CH	3-NH_2, 2-pyrazinyl	122	2,000	490	−0.2
3d	3-aminopropanoyl)piperazin-1-yl	Z = N, X,Y = CH	3-NH_2, 2-pyrazinyl	56	680	180	0.0
3e	(±)-3-(aminomethyl)piperidin-1-yl	Z = N, X,Y = CH	3-NH_2, 2-pyrazinyl	11	700	50	0.5
3f	(*S*)-3-aminopiperidin-1-yl	Z = N, X,Y = CH	3-NH_2, 2-pyrazinyl	16	70	20	0.6
3g	(*S*)-3-aminopiperidin-1-yl	Z = N, X,Y = CH	3-NH_2, 2-pyridyl	18	110	20	1.3

dx.doi.org/10.1021/ml400307j | *ACS Med. Chem. Lett.* 2013, 4, 1193−1197

hetereocycles, which could potentially interact with the protein side chain carboxylates and backbone amides in the ribose patch (Asp128 and Glu171), was targeted. While most modifications offered little if any potency advantage over **3a**, the 3-S amino piperidine compound **3f** stood out with increased potency while further lowering the cLogP to 0.6. From only limited kinase profiling of **3f** it was apparent that the aminopyrazine was fairly promiscuos with its donor and acceptor hinge motif[14] as relative to PIM inhibition several non-PIM kinases were inhibited with equivalent or greater potency.[15] At this time, the unique nature of the PIM hinge was exploited by switching to the donor only C ring aminopyridine **3g**, which maintained comparable PIM potencies relative to **3f**, but with a >100 potency reduction in the non-PIM kinases tested.[16]

From compound **3g** (cLogP = 1.3, $cLogD_{7.4}$ = −0.7), the lower hinge was explored with an eye toward improving potency even if it came at the expense of increased lipophilicity as an ultimate logD7.4 of 1−3 was targeted. The chemistry was amenable to extensive variation (via a C ring 6-bromo-3-aminopyridine) with oxygen, nitrogen, and carbon linkages explored, Table 2. Potency gains were realized as many compounds reached the limits of detection in the low [ATP] assay conditions. Ultimately, the 2,6 difluorophenyl proved highly potent with compound **4j** exhibiting picomolar[17] pan PIM potencies while retaining a reasonable lipophilicity (cLogP = 3.7, $cLogD_{7.4}$ = 1.5). Notably, the panPIM potency increase of **4j** relative to **3g** did not translate into a similar potency increase for the non-PIM kinases tested, as the selectivity window actually widened.[18]

Further optimization of **4j** focused on improving overall drug-like properties, Table 3. Incorporation of a trans hydroxy on the piperidine, **5a**, reduced the lipophilicity while maintaining picomolar pan Pim potency. Attempts to increase potency further with minimal increase in lipophilicity included evaluation of a 5-fluoro substituent on the carboxypyridyl ring as well as targeting a hydrophobic dimple in the glycine loop with additional substituents on the piperidine ring. Incorporation of both of these modifications in the methyl-, hydroxy-, and amino-substitued piperidine **5b** did indeed increase the panPim potency. With the hydroxy addition to the amino-piperidine, it was noted that the PSA, 130, of **5b** as well as number of hydrogen bond donors, six, was increasing. A reduction in both properties was then pursued for potential improvement of overall drug like properties. As the original lead lacked any hinge interaction with PIM kinases, we proceeded to ask the question of whether from these optimized ligands the hinge amino donor interaction could be removed without compromising potency. The hinge donor interaction could indeed be removed without a dramatic loss in potency, as compound **5c** maintained picomolar enzymatic activity and low nanomolar cellular activity, vide infra. When compared alongside the clinical compounds SGI-1776 and AZD1208, **5c** is more potent in enzymatic and cellular, vide infra, assays. As may be expected with no potential hinge interacting moiety, kinase profiling of **5c** using the KINOME scan binding displacement assay indicated high kinase selectivity [$S(35)$ = 0.026 at 1 μM, 442 kinases). With a measured $logD_{7.4}$ of 2.2 and K_is of 1−2 picomolar for PIMs 1−3, the LLE of **5c** is quite high (8.4 with respect to cLogP and 9.2 with respect to measured $logD_{7.4}$).

The crystal structure of **5c** in PIM-1 was obtained, Figure 3.[19] The overall binding mode is the same as the original lead **1a** with the central amide making no hydrogen bonds and displaying the two sides of the molecule toward the hinge/lower hinge and catalytic Lys region/ribose patch. The amino group on the piperidine ring makes two hydrogen bonds to the Asp128 side chain carboxylate and the Glu171 backbone

Table 2. Selected SAR for R1 Analogues of 3g

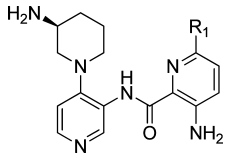

compd	R1	PIM1 K_i (nM)	PIM2 K_i (nM)	PIM3 K_i (nM)	cLogP
3g	hydrogen	18	110	20	1.3
4a	phenyoxy	4	122	15	3.4
4b	2-pyridyl	<1[a]	6	3	2.2
4c	3-pyridyl	<1[a]	12	4	2.0
4d	4-pyridyl	<1[a]	6	5	2.0
4e	2-NH_2-4-pyrimidyl	1	16	3	1.2
4f	2-CH_3O-phenyl	<1[a]	8	<1[a]	2.8
4g	2-CF_3-phenyl	3	7	3	4.3
4h	2-Cl-phenyl	<1[a]	<1[a]	<1[a]	3.8
4i	2-F-phenyl	<1[a]	<1[a]	<1[a]	3.5
4j	2,6-diF-phenyl	0.002[b]	0.004[b]	0.006[b]	3.7

[a]KinaseGlow assay detection limit. [b]Data from high [ATP] Alphascreen assay.

Table 3. Selected SAR for Analogues of 4j and Comparison to SGI-1776 and AZD1208

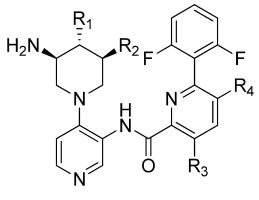

compd	R1	R2	R3	R4	PIM1 K_i (nM)	PIM2 K_i (nM)	PIM3 K_i (nM)	cLogP
4j	H	H	NH_2	H	0.002	0.004	0.006	3.7
5a	OH	H	NH_2	H	0.002	0.006	0.007	2.4
5b	OH	CH_3	NH_2	F	0.001	0.002	0.003	3.1
5c	OH	CH_3	H	F	0.001	0.002	0.001	3.1
SGI-1776					16	610	24	4.6
AZD1208					0.017	0.16	0.23	3.2

dx.doi.org/10.1021/ml400307j | ACS Med. Chem. Lett. 2013, 4, 1193−1197

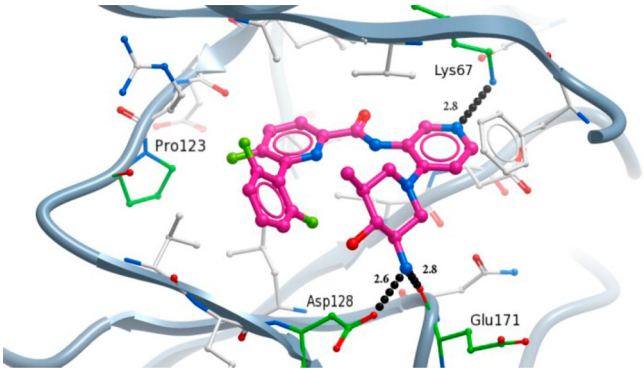

Figure 3. Structure of **5c** in PIM1.

carbonyl in the ribose patch. Additionally, the methyl group fills a hydrophobic dimple in the glycine rich loop above. The B ring pyridine nitrogen makes a hydrogen bond with the catalytic Lys 67. The C ring fluoropyridine fills the Pro123 hinge region with no hydrogen bond interactions and the difluorophenyl ring extends into the lower hinge region.

The picomolar enzymatic PIM activity of **5a**−**5c** translates to nanomolar cellular activity in mechanism target modulation and antiproliferative cell assays for cell lines dependent on PIM1, 2, or 3. For example, in the multiple myeloma derived KMS-11 luc cell line with high expression levels of PIM2, compound **5c** inhibits phosphorylation of pBAD ^{Ser112} (a direct substrate) at 10 nM, inhibits phosphorylation of pS6RP $^{Ser240/4}$ (a downstream substrate) at 38 nM and inhibits cell proliferation at 17 nM.[12] The large upward potency shift in going from the enzyme to cells was consistent with the low ATP K_m for PIM2.[20] In comparison, SGI1776 and AZD1208 inhibit cell proliferation in the KMS-11luc cell line at 4500 and 680 nM, respectively. In the acute myeloid leukemia derived EOL-1 cell line,[21] compound **5c** inhibits cell proliferation at <40 nM.

As a highly kinase selective and cell active pan-PIM inhibitor, compound **5c** was next assessed for it is potential to serve as a tool to study the effect of PIM kinase inhibition in vivo. The close focus on controling lipophilicity during potency optimization proved beneficial as **5c** did indeed possess suitable in vivo properties. Upon dosing 5 mg/kg IV and 10 mg/kg PO of **5c** to mice, a CL of 25 mL/min/kg, a bioavailabity of 55% and a Vss of 4 L/kg were determined. Upon dosing 10 mg/kg IV and 20 mg/kg PO of **5c** to rats, a CL of 13 mL/min/kg, a bioavailabity of 44%, and a Vss of 3.4 L/kg were determined. The favorable physical properties of **5c** were further reflected in the ability to conduct the in vivo studies using acetate buffer formulations. At higher oral doses in both species (up to 100 mg/kg) the plasma exposure increased in a roughly proportional manner relative to the screening PK studies, vide infra. As such, free plasma levels of **5c**[22] in excess of the cellular target modulation and antiproliferative EC_{50}s can be achieved and maintained in rodents.

The target modulation and antiproliferative activity of **5c** in a multiple myeloma (KMS-11.luc) tumor xenograph model has been recently reported.[12] Continual modulation of target, as judged by pS6RP inhibition, was associated with maximal efficacy. In addition to antitumor activity in the multiple myeloma model, here we demonstrate efficacy in the EOL-1 acute myeloid leukemia xenograph model. Administration of **5c** at 30 and 100 mg/kg daily yields significant dose-dependent reduction in tumor growth, Figure 4. Both doses tested were well tolerated, as judged by minimal body weight loss (within a margin of 5% of initial weight) observed for both groups.

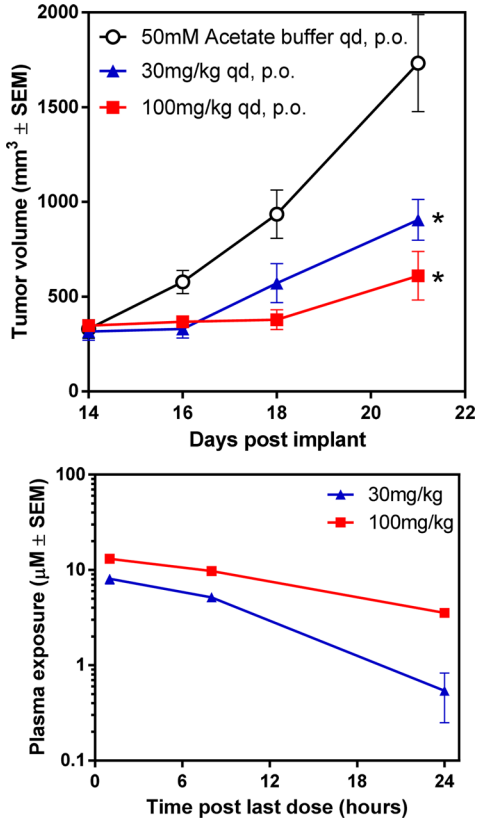

Figure 4. Antitumor activity and plasma exposure of **5c** in EOL-1 acute myeloid leukemia subcutaneous tumor model.

In summary, the structure guided optimization of singleton screening hit **1a** in which the potency against all three PIM isoforms was increased >10,000-fold, with no increase in lipophilicity, to yield compound **5c** that exhibits single digit picomolar pan PIM potency, high kinase selectivity, and in vivo properties suitable to achieve efficacy in an acute myeloid leukemia PIM-dependent tumor model has been described. During the optimization, a focus was initially placed on increasing potency while simultaneously reducing the lipophilicity, as enthalpic contributors to potency were identified. From this lowered clogP space, a hydrophobic interaction was optimized ultimately yielding compound **5c**. Our continued efforts toward bringing forward selective and potent pan PIM kinase inhibitors to benefit cancer patients will be reported in due course.

■ ASSOCIATED CONTENT

Ⓢ Supporting Information

Experimental details for the synthesis and characterization of all compounds, biological assays, and pharmacology model procedures. This material is available free of charge via the Internet at http://pubs.acs.org.

■ AUTHOR INFORMATION

Corresponding Author

*(M.T.B.) E-mail: matthew.burger@novartis.com.

Notes

The authors declare no competing financial interest.

■ ACKNOWLEDGMENTS

We thank Weiping Jia, Dahzi Tang, and Gavin Dollinger for analytical chemistry support.

■ ABBREVIATIONS

AML, acute myeloid luekemia; ATP, adenosine triphospate; [ATP], ATP concentration; BAD, pro-apoptotic protein of the BCl2 family; cLogP, log of the calculated octanol−water partition coefficient of a compound; CL, clearance; FQ, fit quality = LE/LE_Scale; JAK/STAT, Janus Kinase and Signal Transducer and Activator of Transcription; K_m, Michaelis constant; LE, ligand efficiency = ΔG/number of heavy atoms; LLE, ligand lipophilicity efficiency = pKi-clogP; $logD_{7.4}$, log of the octanol−water distribution coefficient at pH 7.4 of ionized and unionized compound; PD, pharmacodynamics; PIM, proviral insertion of Moloney virus; PK, pharmacokinetics; PSA, polar surface area; S6RP, ribosomal protein S6; S(35), number of nonmutant kinases tested with >/65% inhibition/number nonmutant kinases tested

■ REFERENCES

(1) Brault, L.; Gasser, C.; Bracher, F.; Huber, K.; Knapp, S.; Schwaller, J. PIM serine/threonine kinases in the pathogenesis and therapy of hematologic malignancies and solid cancers. *Haematologica* **2010**, *95*, 1004−1015.

(2) Nawijn, M. C.; Alendar, A.; Berns, A. For better or for worse: the role of Pim oncogenes in tumorigenesis. *Nat. Rev. Cancer* **2011**, *11*, 23−34.

(3) Blanco-Aparicio, C.; Carnero, A. Pim kinases in cancer: diagnostic, prognostic and treatment opportunities. *Biochem. Pharmacol.* **2013**, *85*, 629−643.

(4) Jackson, L. J.; Pheneger, J. A.; Pheneger, T. J.; Davis, G.; Wright, A. D.; Robinson, J. E.; Allen, S.; Munson, M. C.; Carter, L. L. The role of PIM kinases in human and mouse CD4+ T cell activation and inflammatory bowel disease. *Cell. Immunol.* **2012**, *272*, 200−213.

(5) Morwick, T. Pim kinase inhibitors: a survey of the patent literature. *Expert Opin. Ther. Pat.* **2010**, *20* (2), 193−212 and references therein.

(6) Mumenthaler, S. M.; Ng, P. Y.; Hodge, A.; Bearss, D.; Berk, G.; Kanekal, S.; Redkar, S.; Taverna, P.; Agus, D. B.; Jain, A. Pharmacologic inhibition of Pim kinases alters prostate cancer cell growth and resensitizes chemoresistant cells to taxanes. *Mol. Cancer Ther.* **2009**, *8*, 2882−2893.

(7) Dakin, L. A.; Block, M. H.; Chen, H.; Code, E.; Dowling, J. E.; Feng, X.; Ferguson, A. D.; Green, I.; Hird, A. W.; Howard, T. Discovery of novel benzylidene-1,3-thiazolidine-2,4-diones as potent and selective inhibitors of the PIM-1, PIM-2, and PIM-3 protein kinases. *Bioorg. Med. Chem. Lett.* **2012**, *22*, 4599−4604.

(8) Haddach, M.; Michaux, J.; Schwaebe, M. K.; Pierre, F.; O'Brien, S. E.; Borsan, C.; Tran, J.; Raffaele, N.; Ravula, S.; Drygin, D. Discovery of CX-6258. A potent, selective, and orally efficacious pan-PIM kinase inhibitor. *ACS Med. Chem. Lett.* **2012**, *3*, 135−139.

(9) Nishiguchi, G. A.; Atallah, G.; Bellamacina, C.; Burger, M. T.; Ding, Y.; Feucht, P. H.; Garcia, P. D.; Han, W.; Klivansky, L.; Lindval, M. Discovery of novel 3,5-disubstituted indole derivatives as potent inhibitors of Pim-1, Pim-2, and Pim-3 protein kinases. *Bioorg. Med. Chem. Lett.* **2011**, *21*, 6366−6369.

(10) Wang, X.; Magnuson, S.; Pastor, R.; Fan, E.; Hu, H.; Tsui, V.; Deng, W.; Murray, J.; Steffek, M.; Wallwever, H.; Moffat, J.; Drummond, J.; Chan, G.; Harstad, E.; Eben, A. J. Discovery of novel pyrazolo[1,5-a]pyrimidines as potent pan-Pim inhibitors by structure- and property-based drug design. *Bioorg. Med. Chem. Lett.* **2013**, *23*, 3149−3153.

(11) Qian, K. C.; Wang, L.; Hickey, E. R.; Studts, J.; Barringer, K.; Peng, C.; Kronkaitis, A.; Li, J.; White, A.; Mische, S.; Farmer, B. Structural basis of constitutive activity and a unique nucleotide binding mode of human Pim-1 kinase. *J. Biol. Chem.* **2005**, *280*, 6130−6137.

(12) Lu, J.; Zavorotinskaya, T.; Dai, Y.; Niu, X.; Castillo, J.; Sim, J.; Yu, J.; Wang, Y.; Langowski, J. L.; Holash, J.; Shannon, K.; Garcia, P. D. Pim2 is required for maintaining multiple myeloma cell growth through modulating TSC2 phosphorylation. *Blood* **2013**, *122*, 1610−1620.

(13) Structure of **1a** in PIM1 submitted under PDB accession code 4N6Y.

(14) The hinge binding potential of **3f** was confirmed by the X-ray cocrystal in Pim1, submitted under PDB accession code 4N6Z.

(15) PDGF(0.009 μM), PKCε(0.014 μM), PKCδ(0.032 μM), and PKA (0.15 μM).

(16) PDGF(1.7 μM), PKCε(3.9 μM), PKCδ(14 μM), and PKA (>25 μM).

(17) With compound potency at the limit of detection, assay format changed to high [ATP]. See Supporting Information.

(18) PDGF(0.30 μM), PKCε(9.3 μM), and PKA (8.9 μM).

(19) Structure of **5c** in PIM1 submitted under PDB accession code 4N70.

(20) Pim1, 2, and 3 exhibit 400, 4, and 40 μM ATP K_ms. On the basis of Cheng−Prusoff equation, a ca. 12.5-, 1250-, or 125-fold shift, respectively (assuming 5 mM cellular ATP concentration), is to be expected from enzymatic K_is to target modulation EC_{50}s.

(21) Mayumi, M. EoL-1, a human eosinophlic cell line. *Leuk. Lymphoma* **1992**, *7*, 243−250.

(22) Mouse and rat plasma protein binding of **5c** are 98% and 97%, respectively.